PERGAMON

International Journal of Heat and Mass Transfer 43 (2000) 1925–1934

International Journal of HEAT and MASS TRANSFER

www.elsevier.com/locate/ijhmt

Characteristics of liquid–wall contact in post-CHF flow boiling

Asuman F. Cokmez-Tuzla*, Kemal Tuzla, John C. Chen

Institute of Thermo-Fluid Engineering and Science, 111 Research Drive, Bethlehem, PA 18015, USA

Received 16 February 1999; received in revised form 1 September 1999

Abstract

In several industrial applications, highly heated metal channels are quenched by advancing fronts of cold liquid. The transient heat transfer in the vicinity of the advancing quench front governs the dynamics of the overall process, controlling the rate of quench front advancement. Most analyses to date assume that the hot metal in front of the quench front is above the Leidenfrost temperature and cannot sustain direct liquid contacts. This investigation sought to experimentally assess the validity of the no-contact assumption, and to record specific characteristics of such contacts if they occur. In order to detect and record potential liquid contacts in the vicinity of an advancing quench front, a special rapid-response probe was utilized. Tests were carried out with water at atmospheric pressure and over a range of wall superheats and quench front propagation velocities. Analysis of the experimental data provided information on the probability, duration, and time fraction of liquid contacts as functions of wall superheat and distance from the quench front.

Keywords: Transition boiling; Film boiling; Liquid–wall contact; Post-CHF heat transfer

1. Introduction

The prediction of the heat transfer of quenching on metal surfaces that are at temperatures higher than the saturation temperature of the flowing liquid (from now on called "superheated metals") is an important aspect for boiling systems, cryogenic systems, metallurgical processing, steam generators and many other applications. It is especially important in the safety analysis of nuclear power plants where water is used to cool high-temperature fuel rods. Heat transfer from the hot wall to the two-phase flow can either be transmitted from the wall to the vapor or from the wall to the liquid. Due to temperatures involved, radiation heat transfer is often negligible in these cases. Many investigators assumed a priori that liquid contact is not possible on highly superheated surfaces and chose to ignore the possibility of transient conduction to impacting drops [1,2]. Other investigators argued that droplets can approach close to the heated surface, but will be deflected by evaporating vapor [3]. More general models, notably that of Iloeje et al. [4] and Chen et al. [5] include the possibility of direct heat transfer to impinging drops. However, due to a lack of definitive experimental information, such formulations are forced to various levels of empirical "guess work" in describing such liquid–wall heat transfer.

Previous studies to measure liquid–wall contacts were concentrated mostly on the transition region in

* Corresponding author. Tel.: +1-610-758-4729; fax: +1-610-758-5057.

E-mail address: kt01@lehigh.edu (A.F. Cokmez-Tuzla).

0017-9310/00/$ - see front matter
PII: S0017-9310(99)00274-4

Nomenclature

CHF	critical heat flux
F_L	liquid contact fraction
G	mass flow rate
ICT	integrated contact time
p	pressure
q	heat flux
t	time
T	temperature
ΔT_w	$T_w - T_s$ wall superheat
V_q	velocity of dry-out point
x	thermodynamic quality of liquid/vapor flow
z	elevation from the test section lower flange

Subscripts

q	quench
in	inlet
L	liquid
S	saturation
v	vapor
w	wall

pool boiling without the forced flow of a quenching fluid. Dhuga and Winterton [6] and Rajabi and Winterton [7] used impedance probes to measure liquid contact fractions in the transition pool boiling of water and methanol. Jarman et al. [8] developed an ultrasonic probe to detect direct liquid contacts with the wall for the pool boiling of R-113 refrigerant, again in the transition regime. Lee et al. [9] and Shoji et al. [10] used micro thermocouples to detect liquid–wall contacts in the pool boiling of water. In flow boiling, however, there are only a few known experimental studies. Ragheb and Cheng [11] measured the fraction of the surface that was wetted during the quenching of a thick copper block under flow boiling conditions by using an electrical conductance probe. They used water at atmospheric pressure as the working fluid and their experiments were conducted at low wall superheats. In another study, Chang and Witte [12] used a micro thermocouple to detect liquid–solid contacts during a cross flow of R-11 over a cylindrical rod. Finally, in a recent study, the present authors [13,14] experimentally verified the presence of liquid–wall contacts in post-CHF flow boiling. The objective of the present study was to determine some of the quantitative characteristics of liquid–wall contacts in the vicinity of quench fronts for flow boiling, with emphasis on the time fraction of contacts.

2. Experiment

A schematic drawing of the two-phase heat transfer loop is shown in Fig. 1. The tubular test section was made of an Inconel tube of 1.57 cm ID and 172 cm length. The test section was directly heated by sending a current through the conductive tube wall. A copper hot-patch was used at the top of the test section to prevent quenching from the top. The wall temperatures at 26 different axial locations were measured by chromel–alumel thermocouples attached to the outside surface of the tube.

A contact probe, which is a fast response surface temperature thermocouple, was developed to measure liquid contacts with the wall [13]. During the experiments the 3.1 mm OD contact probe was mounted flush with the inside surface of the test tube as shown in Fig. 2(a). The layer that formed the thermocouple junction was measured to be about 5–8 μm as shown in Fig. 2b. Thus the probe detected liquid induced cooling by tracking transient temperatures approximately 16 μm beneath the surface. The response time of this probe was determined to be better than 0.1 ms to sense 99% of any sudden temperature change. Further details of the probe, the test section, and the two-phase loop are given in Refs. [14,15].

At the start of an experiment, the test section would be preheated to superheat temperatures in the range of 400–500°C, while the two-phase flow was bypassed around the test section. During this preheating period, the two-phase flow was adjusted to the desired mass flux and equilibrium quality by controlling the pump and the heating power to the flow. After the desired conditions were reached, the fluid was diverted from the bypass line into the bottom of the test section, establishing an initial quench front close to the bottom inlet of the test section. Since input heating to the tube was small compared to the rate of heat removal at the quench front, the tube wall around the quench front cools and the quench front propagates slowly upward into the test section. This slowly moving quench front leads to the pseudo-steady-state thermal hydraulic conditions further downstream of the quench front. During the propagation process, wall temperatures along the test section, heat inputs to the boiler and test section, liquid flow rate, and inlet and outlet temperatures of the test fluid were recorded by a process data logger. A separate high speed data acquisition system simultaneously recorded output signal from the contact

probe at a frequency of 16,000 data points per second, giving a resolution better than 0.1 ms. Water was used as the working fluid under the following operating conditions:

G = 9–31 kg/m^2 s
x_{in} = 10°C subcooled — 0.25 vapor quality
p = 103 kPa
q = (1.5 – 5.5) 10^4 W/m^2
ΔT_w = up to 500 K

3. Test results

The results from the experimental tests are reported in the following section, with the operating conditions of these tests outlined in Table 1.

The overall quenching process is described in Figs. 3–5 by studying the variations in the wall temperatures as the quench front moved along the tube. Axial variation of measured wall temperatures are shown in Fig. 3 for three different times during a typical experiment. The horizontal axis shows the elevation measured from the test section inlet. For a given time, t_1, the wall temperatures stay close to the saturation temperature at lower elevations, indicating a high heat transfer coefficient between the wall and the fluid. Therefore this region corresponds to convective nucleate boiling with heat transfer directly from the wall to the liquid. At higher elevations (between 20 and 40 cm), wall temperatures suddenly increase from 120°C to 400°C within a short ($\approx$10 cm) distance, indicating a dry-out of the test section or lack of liquid contact with the wall. After dry-out, heat transfer is limited by the presence of convective film boiling and the wall temperature continues to rise at a slow rate. Since the wall heat flux is kept at lower values than is required to stop the quenching of the test section, the quench front will progress upward and eventually cool the wall. This is seen again in Fig. 3 where axial temperature profiles at two different times after t_1, are shown. Thus, the wall temperature at a fixed elevation will decrease with time and eventually will quench to the temperature of the liquid as presented in Fig. 4. Variation of wall temperature with time is shown in this figure for two different elevations. The two solid lines represent measured wall temperatures for elevations of 700 and 800 mm. Initially, the dry-out point is below these elevations; therefore, wall temperatures at these elevations are at high superheat, corresponding to post critical heat flux conditions. As the dry-out point progresses upward, the wall cools down slowly in the film boiling region. Later, as the dry-out point gets closer,

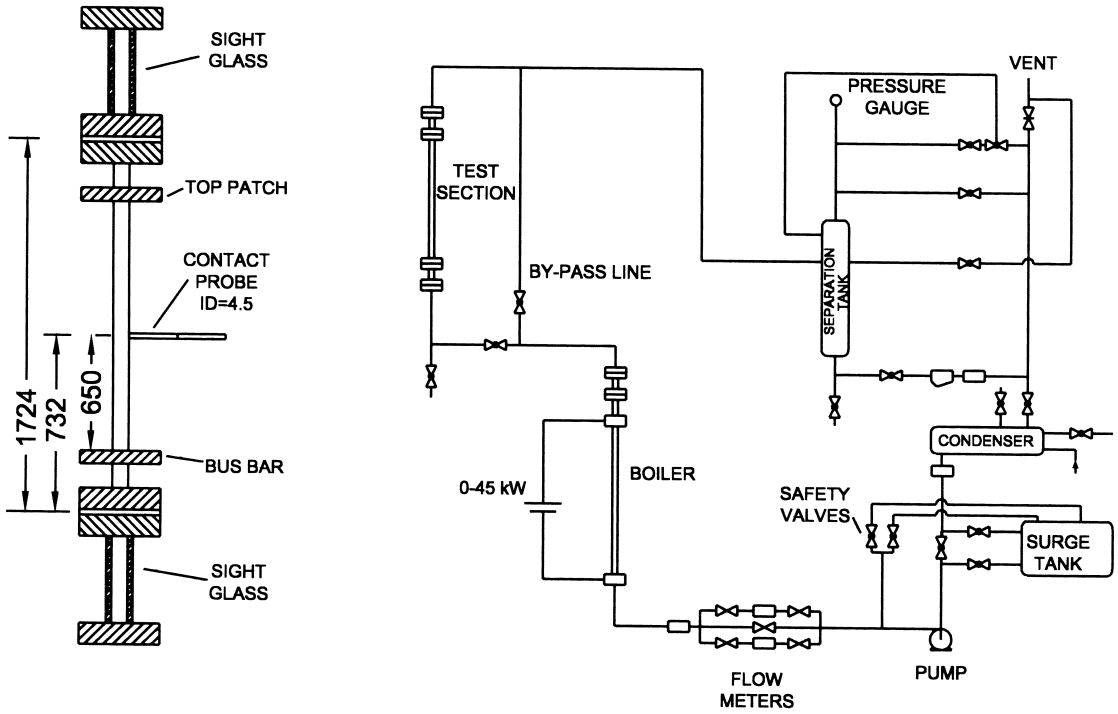

Fig. 1. Schematic of the two-phase test loop and the test section.

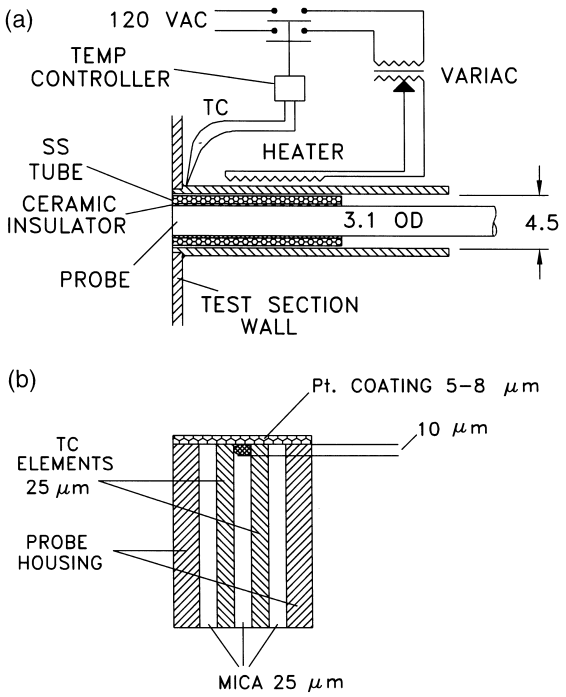

Fig. 2. (a) Schematic of mounting of the contact probe onto the test section wall. (b) Schematic of sensing tip of the contact probe thermocouple.

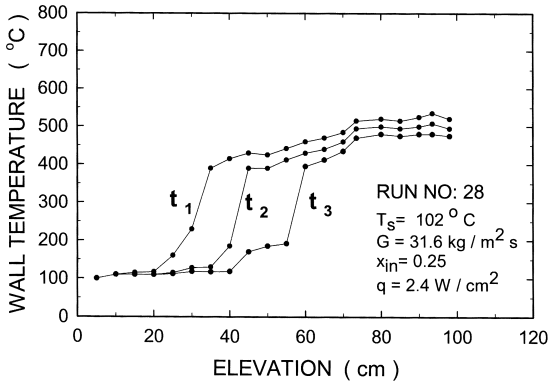

Fig. 3. Axial variation of wall temperature at three different times during a reflood test.

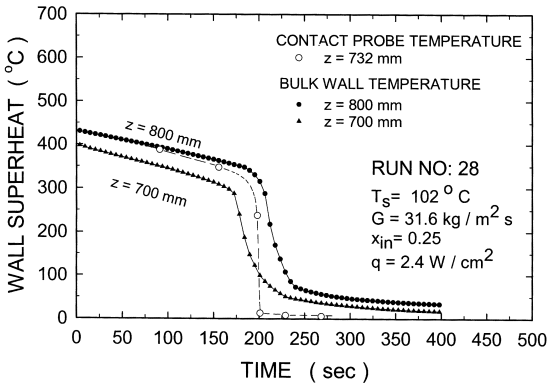

Fig. 4. Variation of wall temperature with time as measured by the contact probe and by two wall thermocouples.

the rate of decrease in the wall temperature increases and reaches a maximum. The CHF point corresponds to the inflection point on the temperature curve when the wall is going through a quench [16]. After this point, the heat transfer is by nucleate boiling where the wall temperatures stay close to the saturation temperature of the fluid. The points shown with the white circles in Fig. 4 are surface temperatures measured by the contact probe, which is located between these two elevations (i.e. the contact probe is located at 73.2 cm elevation). It is seen that, at times earlier than the rapid quench transient, the contact probe temperatures are between the bulk wall temperatures measured by the thermocouples attached to the wall, for the 70 and 80 cm elevations. This indicates that the presence of the contact probe and its port did not affect the thermal hydraulic behavior in the test channel. Once the rapid transient starts, the contact probe responds much faster than the bulk wall thermocouples. As a result, the contact probe measures lower temperatures

Table 1
Operating conditions of reflood tests

Run	T_s (°C)	G (kg/m^2 s)	x_{in}	x_q	q (W/cm^2)	V_q (m/s)	$G_{v,q}$ (kg/m^2 s)	$G_{L,q}$ (kg/m^2 s)
12	101	12.8	0.24	0.361	1.96	8.00	4.62	8.18
14	101	12.9	0.09	0.217	2.08	5.58	2.80	10.10
25	101	12.9	0.01	0.229	3.58	5.57	2.95	9.95
27	102	31.7	0.25	0.305	2.23	16.40	9.67	22.0
28	102	31.6	0.25	0.310	2.40	16.86	9.80	21.8
29	102	31.8	0.09	0.155	2.61	9.53	4.93	26.9

after 200 s for this sample run. The quenching times for each elevation were calculated as described above and plotted in Fig. 5. It is seen that for this sample test run, the quench front progresses upward with a slowly increasing speed. For the conditions of the present run, the quench velocity varied from 2.33 mm/s at lower elevations to 3.33 mm/s at higher elevations.

The contact probe signal was recorded from the start to the end of a run, which on the average took about 8–10 minutes, totaling about 8×10^6 data points per run. The raw signal showed some high frequency fluctuations due to electronic noise generated by the electrical heating of the test tube and the probe port. The frequency of the noise was found to be 360 Hz and were subsequently removed from the data by using Fast Fourier transforms with low pass filtering (eliminating frequencies higher than 220 Hz). This filtering process removed the periodic noise but did not alter the significant temperature variations indicated by the signal.

A sample of a contact probe signal after filtering is shown in Fig. 6(a) for an entire quench transient. The vertical axis represents the wall surface superheat and the horizontal axis shows the test time. The signal indicates that the temperature of the probe tip initially stayed at high superheats of about 300–400°C (region A) and decreases gradually with intermittent sudden drops and recoveries. This region clearly corresponds to the film boiling regime. As the quench front approached the location of the probe, the wall temperature dropped at a fast rate (region B), indicating quenching of the wall at the probe location. This region, with its large temperature drops and recoveries, indicates a transition boiling mechanism. Finally, during the remainder of the test (region C), the wall temperature stayed close to the saturation temperature representing convective nucleate boiling.

If a portion of the signal in Fig. 6(a) (region D) is expanded in both time and temperature scales, the liquid contacts can be seen more clearly, as shown in Fig. 6(b). In this expanded scale, the sudden temperature drops, up to 15°C for this sample, clearly indicate a high cooling mechanism even at this high wall superheat of 320°C. Next, Fig. 6(c) shows in further detail, the first three quenching contacts of Fig. 6(b) (region E). It is seen that sudden surface temperature drops continue for tens of milliseconds. Finally, the data are further expanded in Fig. 6(d) to magnify only one contact (region F), to the point where individual data points are almost discernable at an interval of only 0.0625 milliseconds. The figure shows that the wall temperature is almost constant at times before point G. Right after this point, the surface is cooled with a temperature drop rate of 4050°C/s (between points G and H). Later, the temperature drop rate is reduced to 760°C/s between points H and I. Finally, at times after the point I, the surface temperature recovers toward the initial value. It is hypothesized that the fast cooling of the surface between points G and I is due to cooling by a liquid droplet which is in contact with the wall. This hypothesis was examined and verified by using the transient conduction analysis described in [14]. Our interpretation is that liquid–wall contact starts when the rapid decrease in wall temperature begins (point G), and ends when the wall temperature begins to recover (point I). Further discussion about precise locations of start and end points of contact is presented below.

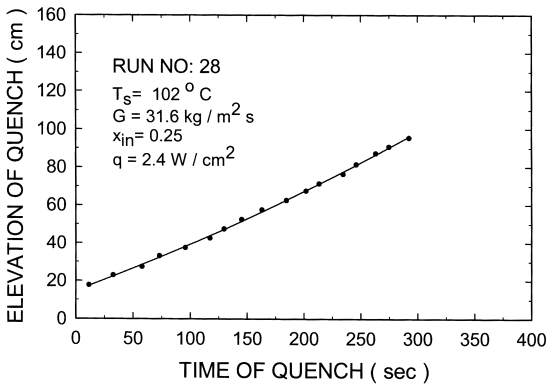

Fig. 5. Progress of quench front during a reflood test.

3.1. Contact criteria limits

It is seen from Fig. 6 that there were many contacts similar to the one shown in Fig. 6(d), while the quench front was approaching the probe location. All of the contacts observed in Fig. 6 showed similar behavior. Based on these observations and calculations described in [14], the following criteria were selected to define liquid contacts.

A. To start a contact:

1. The probe temperature must drop more than the random deviation on the temperature signal. During vapor contact of the wall the random deviation on wall temperature is less than 1°C. Therefore, this limit for minimum temperature drop is selected as 1°C.
2. The rate of continuous temperature drop must be greater than 1000°C/s, indicating high cooling rates associated with liquid contacts.

When both criteria are satisfied, it is assumed that there is a liquid contact on the wall.

B. To end a contact:

1. The probe temperature must go through a minimum and start to rise.

2. The continuous recovery of the probe temperature must be greater than the standard deviation on the data. This limit is 1°C for high wall superheats (i.e. wall superheats greater than 50°C) and 14°C for low wall superheats (i.e. wall superheats less than 50°C)
3. Contact ends when the transient temperature–time history reaches its inflection point.

Further discussion on selection of the above criteria are provided in [14] and [15].

Since the tests deal with a large number of data points, a computer program was developed to detect the time intervals when the liquid is in contact with the surface (i.e. droplet residence time or contact duration). Results show that the liquid contacts occur in a random nature. Thus, liquid contacts with the wall are grouped according to wall temperature and residence time (contact duration). For a given wall temperature and contact duration, the probability of liquid contacts can be defined as the ratio of the number of contacts with a specific residence time during a specific time interval, to the total number of contacts during the same time interval while the wall was at a specific superheat. The probability distribution of the liquid contacts is shown in Fig. 7 for various wall superheats. The horizontal axis represents the residence time of the liquid contacts and the vertical axis represents the probability of contacts. There are seven plots in this figure each representing a range of wall superheats with ± 25°C around a mean. The mean values of these wall superheats are indicated on the right hand side of the horizontal axis. It is seen that most of the contacts occur with residence times between 0 and 15 ms and there are no specific trends with changing wall superheat. The frequencies of these contacts were also calculated at specific wall superheats without considering the residence times, and are shown in Fig. 8. For this specific test run, no contacts were observed at wall

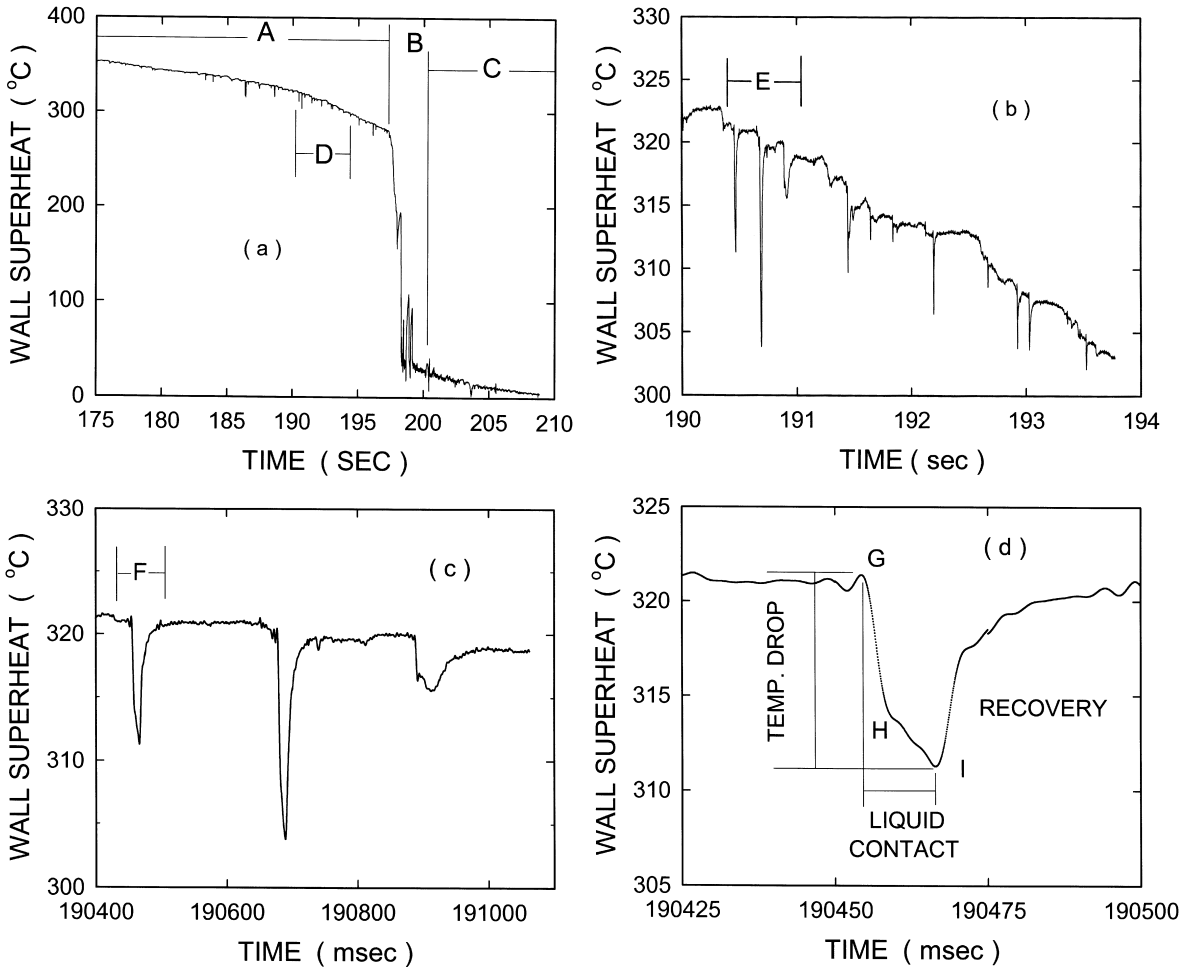

Fig. 6. A sample contact probe signal indicating variation of instantaneous wall surface temperature during a reflood test.

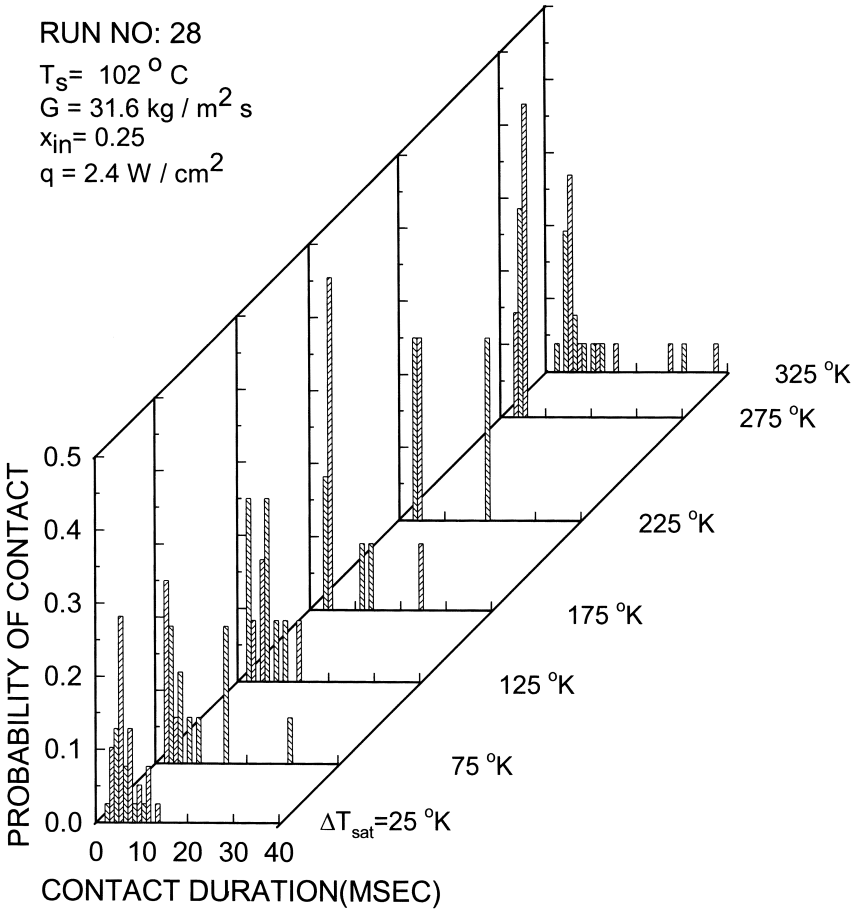

Fig. 7. Probability distribution of contact durations.

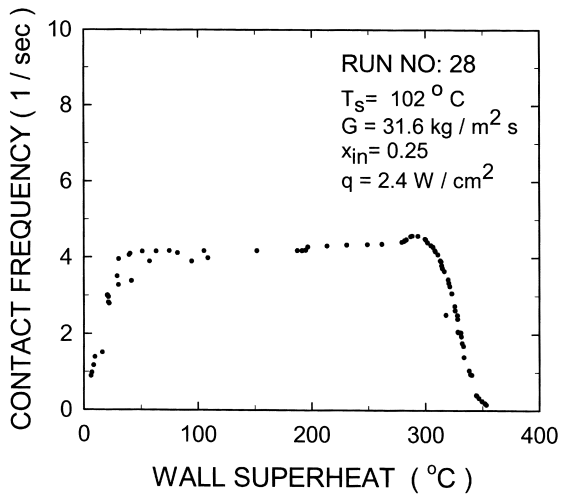

Fig. 8. Frequency of liquid contacts as a function of wall superheat.

superheats higher than 360°C. At wall superheats less than 360°C, the contact frequency increased sharply and stayed constant at slightly above 4 Hz until nucleate boiling conditions were reached at low wall superheats indicated by a decline in contact frequency to continuous liquid contact. Similar results were obtained in all test runs conducted.

3.2. Calculation of liquid contact fraction, F_L

The liquid contact fraction is defined as the ratio of the duration of liquid contact to the total time when both liquid and vapor contacts the wall. This is described in Fig. 9 for a generic case with periodic contacts. For the conditions of the present study, the liquid–wall contacts do not happen in a uniform and periodic fashion as was shown in Fig. 6. This is mostly due to the random nature of the phenomena and partly due to the changing test conditions with time. Keeping this in mind, an averaging procedure

described below was used in the present work. The procedure consists of the following steps.

1. Actual time of contact (t_i) and contact duration ($t_{c,i}$) of each liquid contact are determined as sketched in Fig. 9.
2. Summation of these contact durations give the integrated contact time as:

$$\mathrm{ICT}(t) = \int_0^t \delta \, \mathrm{d}t \tag{1}$$

where $\delta = 0$ during vapor contact and $\delta = 1$ during liquid contact.

Integrated contact time (ICT) calculated for a sample case is shown in Fig. 10(a). The data for ICT shows two distinct regions. In the first region, between 170 and 197 s, ICT increases with a slowly increasing rate. In the second region, at times after 197 s, ICT increases linearly with time with a gradient equal to unity. The first region corresponds to a post-CHF zone where liquid contacts with the wall are intermittent. The second region corresponds to nucleate boiling where liquid contact on the wall is continuous. The solid line in this figure indicates a curve fit to the data. This function was selected to represent the expected behavior, i.e., (a) ICT must continuously increase with increasing time and (b) the gradient must reach unity in the second region where the data shows continuous contact.

3. Based on the above definitions, the derivative of ICT with respect to time will give the time fraction of liquid contact, i.e.,

$$F_L = \frac{\mathrm{d}(\mathrm{ICT})}{\mathrm{d}t} \tag{2}$$

For the sample case used in Fig. 10(a), calculated F_L values are shown in Fig. 10(b) as a function of time. As expected, at early times contact fractions are very low (close to zero), increase with increasing time and finally reach unity as the quench front arrives at the probe location.

The information in Fig. 10(b) was combined with the wall temperature data of Fig. 6(a) to cross plot F_L as a function of wall superheat. This is shown in Fig. 11(a) for this sample case. The wall superheats reported in this figure are the measured wall superheats at the beginning of each contact. It is seen from Fig. 11(a) that at about 360°C wall superheat, F_L is much less than 0.01. With decreasing superheat F_L increases sharply until about 280°C. Between 280°C and 20°C,

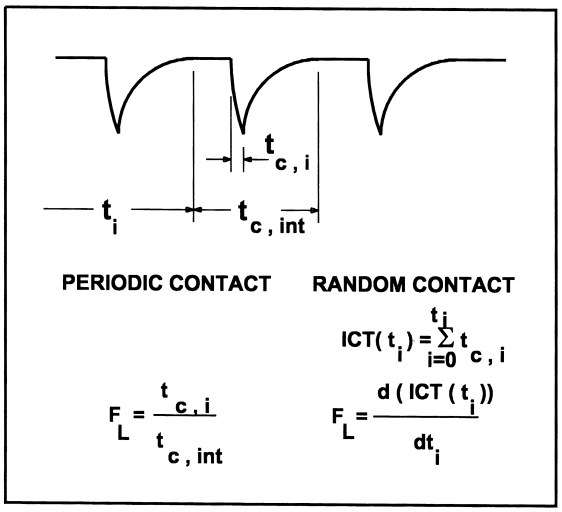

Fig. 9. Definition of F_L for idealized (periodic) and random contacts.

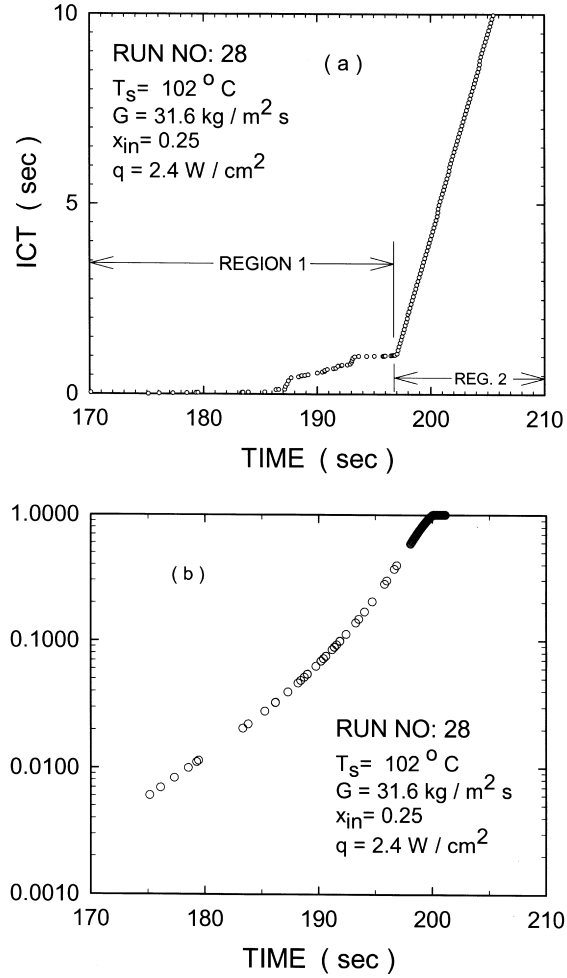

Fig. 10. Variation of ICT and F_L with time for a sample test case.

F_L stays at high values (~0.65), and then increases to unity at wall superheat temperatures of less than 20°C.

Similarly, F_L values were also evaluated as a function of distance from the dry-out location by using the information given in Fig. 5. This is shown in Fig. 11(b), where the horizontal axis represents the distance between the probe location and dry-out point. As expected, F_L is equal to unity at the dry-out point and decreases with increasing downstream distance. For the conditions of the sample test, it is seen that liquid contact fraction is 10% at a distance of 25 mm and 1% at 65 mm distance from the dry-out point.

Variation of F_L with wall superheat temperatures is shown in Fig. 12 for six different runs. The data show a similar trend for all of the runs, that is, at high wall superheats F_L increases with decreasing wall superheat, then reaches a plateau between wall superheats of 20–280°C and finally increases to unity with further decrease in wall superheat. At wall superheats between 280 and 400°C, the data for most of the test runs gather within ±20°C wall superheat showing quite a good agreement. Furthermore, none of the data showed liquid contact at wall superheats of higher than 400°C. For wall superheats between 20 and 280°C, the data show uniform contact fractions. In this temperature region the magnitude of F_L varies from less than 0.1 for runs 12 and 14 to more than 0.50 for runs 27, 28 and 29. Further analysis of the data showed that the amount of liquid at dry-out point was higher for runs 27, 28 and 29 than the others. Table 1 indicates that liquid flux around the dry-out point was between 22 and 27 kg/m^2 s for runs 27, 28 and 29, and about 10 kg/m^2 s for runs 12 and 14. Thus, it can be concluded that for a given wall superheat between 20 and 280°C, F_L increases with increasing liquid flux. Variation of F_L with distance

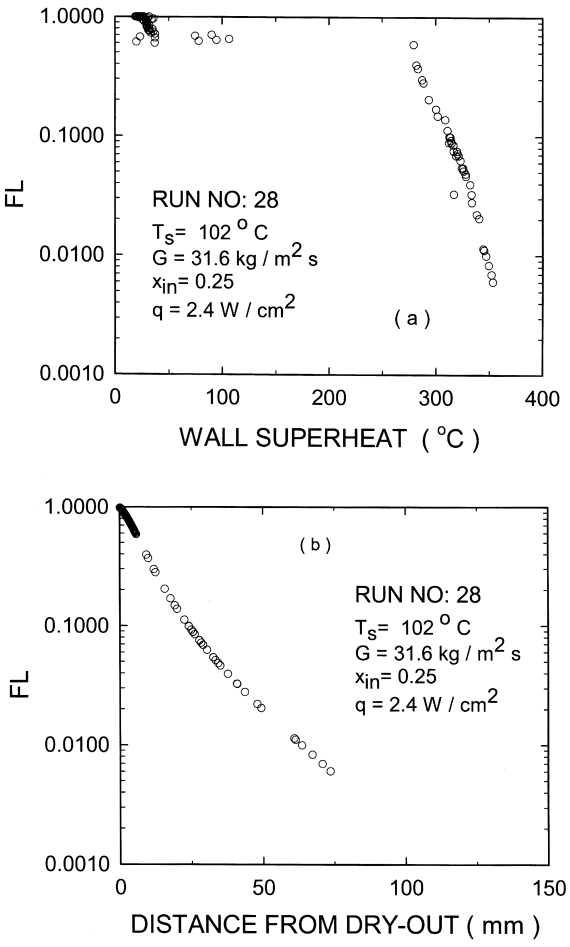

Fig. 11. Variation of F_L with wall superheat and distance for a sample case.

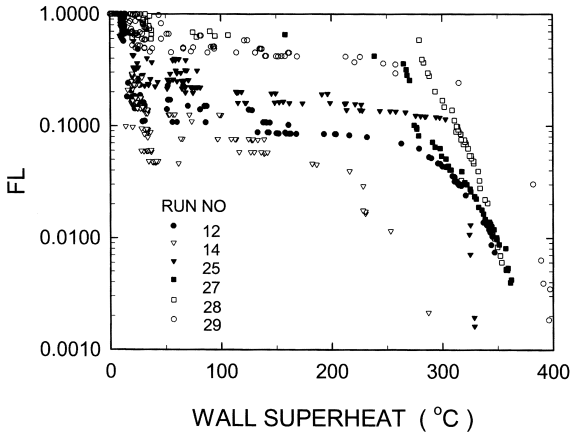

Fig. 12. Variation of F_L with wall superheat for all tests.

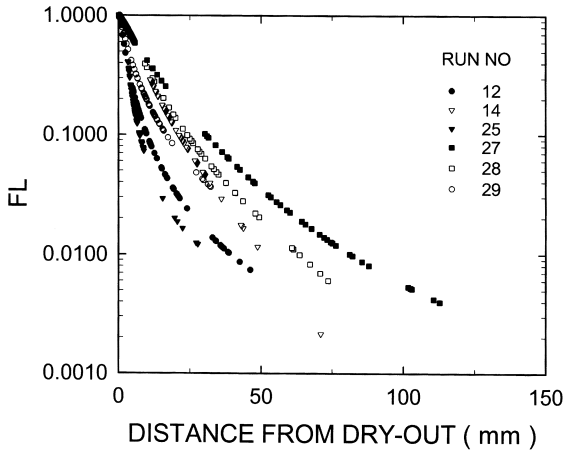

Fig. 13. Variation of F_L with distance from the dry-out for all tests.

from dry-out is shown in Fig. 13 for all the test runs. The data show a decreasing F_L with increasing distance from the dry-out location. The effective length, where there are liquid contacts, varies from 50 mm to 120 mm for the conditions of these tests. It is also observed that test runs with lower liquid flux (i.e. runs 12, 25 and 14) show shorter effective near field lengths than test runs with higher liquid flux (i.e. runs 27 and 28). It is expected that this length with liquid contacts represent the near field region where there is a high vapor generation due to direct wall to liquid heat transfer. It is also expected that this length with liquid contacts will increase with increasing mass flux.

4. Conclusions

Characteristics of liquid–wall contacts were investigated for quenching of superheated channels. Experimental test results indicated that liquid droplets can contact the hot walls at wall superheat temperatures up to 400°C, although liquid–wall contact durations were found to be no longer than 25 ms. Liquid contact fractions decreased with increasing distance from the dry-out location, increasing wall temperatures and decreasing liquid mass flux.

References

[1] R.S. Dougal, W.M. Rohsenow, Film boiling on the inside of vertical tubes with upward flow of the fluid at low qualities, MIT-TR-9079-26, MIT, Boston, MA, 1963.

[2] K.G. Condie, S.J. Bengston, S.L. Richlein, Post-CHF heat transfer data-analysis, comparison and correlation, unpublished report, Idaho National Engineering Laboratory, Idaho Falls, ID, 1974.

[3] A.F. Varone Jr, W.M. Rohsenow, Post-dryout heat transfer prediction, in: Proceedings of The First International Workshop on Fundamental Aspects of Post-Dryout Heat Transfer, NUREG/CP-0060, NRC, Washington, DC, 1984, pp. 457–484.

[4] O.C. Iloeje, D.N. Plummer, W.M. Rohsenow, P. Griffith, An investigation of the collapse and surface rewet in film boiling in forced vertical flow, Journal of Heat Transfer 97 (1975) 166–172.

[5] J.C. Chen, R.K. Sundaram, F.T. Ozkaynak, A phenomenological correlation for post-CHF heat transfer, NUREG-0237, NRC, Washington, DC, 1971.

[6] D.S. Dhuga, R.H.S. Winterton, Measurement of surface contact in transition boiling, Int. J. Heat Mass Transfer 28 (1985) 869–1880.

[7] A.A. Alem Rajabi, R.H.S. Winterton, Liquid–solid contact in steady state transition pool boiling, Int. J. Heat and Fluid Flow 9 (1988) 215–219.

[8] D. Jarman, A.N. Sinclair, D. Groeneveld, Ultrasonic measurement of the wetted fraction of a heat transfer surface under pool boiling conditions, Experimental Thermal and Fluid Science 3 (1990) 395–403.

[9] L. Lee, J.C. Chen, R.A. Nelson, Surface probe for measurements of liquid contact in film and transition boiling on high temperature surfaces, Rev. Sc. Instruments 53 (1982) 1472–1476.

[10] M. Shoji, L.C. Witte, S. Yokoya, M. Kawakami, H. Kuroki, Measurement of liquid–solid contact using micro-thermocouples in pool transition boiling of water on a horizontal copper surface, in: Proceedings of the ASME/JSME Thermal Engineering Conference, vol. 2, ASME, New York, 1991, pp. 333–338.

[11] H.S. Ragheb, S.C. Cheng, Surface wetted area during transition boiling in forced convective flow, Journal of Heat Transfer 101 (1979) 381–388.

[12] K.H. Chang, L.C. Witte, Liquid–solid contact during flow film boiling of subcooled Freon-11, Journal of Heat Transfer 112 (1991) 465–471.

[13] A.F. Cokmez-Tuzla, K. Tuzla, J.C. Chen, High speed thermometry for detection of transient liquid contact on superheated surfaces, in: J. Schooley (Ed.), Temperature: its Measurement and Control in Science and Industry, vol. 6, American Institute of Physics, New York, 1993, pp. 1173–1177.

[14] A.F. Cokmez-Tuzla, Investigation of wall to liquid heat transfer in post-CHF flow boiling in a vertical tube, Ph.D. Thesis, Lehigh University, Bethlehem, PA, 1991.

[15] A.F. Cokmez-Tuzla, K. Tuzla, J.C. Chen, Experimental assessment of liquid–wall contacts in post-CHF convective boiling, Nuclear Engineering and Design 139 (1993) 97–103.

[16] D. Evans, S. Webb, J.C. Chen, Axially varying vapor superheats in convective film boiling, Journal of Heat Transfer 107 (1985) 668–669.